

Structural, electrical and optical properties of $\text{Cd}_x\text{Zn}_{1-x}\text{Se}$ thin films

H. S. Soliman¹, N. A. Ali², A. A. El-Shazly¹

¹ Faculty of Education, Ain Shams University, Heliopolis, Roxy, Cairo, Egypt

² Faculty of Science, Helwan University, Egypt

Received: 16 September 1994/Accepted: 3 January 1995

Abstract. X-ray diffraction and electron diffraction techniques indicate that $\text{Cd}_x\text{Zn}_{1-x}\text{Se}$ thin films on glass substrates have a polycrystalline nature, with sphalerite structure for $x \leq 0.5$ and wurtzite structure for $x \geq 0.6$. The crystalline size in each composition increases with increasing the film thickness. The room temperature dark resistivity ρ varies from one composition to another showing a transition at $x = 0.55$.

The temperature dependence of ρ of the deposited films revealed two conduction mechanisms, one below 352 K due to shallow levels, surface states, and defects introduced during the film growth, and over 352 K due to deep-level ionization following the ordinary semiconducting behaviour.

The thermal activation energy of the free charge carriers decreases linearly with increasing the molar fraction x of the CdSe content up to $x = 0.55$, above which it increases with increasing x .

The optical constants of $\text{Cd}_x\text{Zn}_{1-x}\text{Se}$ thin films of different compositions were determined in the spectral range 400–2000 nm. The analysis of the absorption coefficient at and near the absorption edge indicates the existence of allowed direct transition energy gaps decreasing with increasing x .

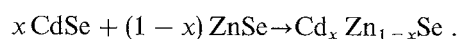
PACS: 78.50

The semiconducting binary compounds CdSe and ZnSe have been used in electronic devices, optical detectors and photovoltaic applications [1–9]. Ternary solid solutions composed from these two compounds are expected to have interesting physical properties. The present work was directed to investigate the structural, electrical, and optical properties of $\text{Cd}_x\text{Zn}_{1-x}\text{Se}$ solid solution in thin film form.

1 Experimental procedure

1.1 Sample preparation

$\text{Cd}_x\text{Zn}_{1-x}\text{Se}$ solid solutions were synthesized from the two binary compounds CdSe and ZnSe according to:



Therefore, stoichiometric amounts of these two constituents were mixed together and fused in evacuated sealed silica tubes at 1273 K for 24 h, after which the tubes cooled at a rate of about 300 K h^{-1} . Following this procedure nine $\text{Cd}_x\text{Zn}_{1-x}\text{Se}$ solid solution ingots with $0.1 < x < 0.9$ were prepared.

Each composition was used in the preparation of a group of thin films of different thicknesses using a single source thermal evaporation technique. The deposition process takes place in vacuum of $2 - 3 \times 10^{-5}$ Torr onto glass or quartz substrates held at room temperature. The film thickness and the deposition rate (0.4 nm s^{-1}) were controlled using a quartz thickness monitor (Edwards, type FTM4) then the film thickness was measured using multiple-beam Fizeau fringes method [10].

1.2 Structural investigation

An X-ray diffractometer (type Philips 1773) provided with Ni-filtered Cu K_{α} radiation was used for investigating the $\text{Cd}_x\text{Zn}_{1-x}\text{Se}$ solid solution in powder form and in thin films form, deposited onto glass substrates. The diffraction patterns were recorded automatically with a scanning speed of 2 degrees per minute and a scanning angular range from 10° to about 90° . The analytical method [11] was utilized for indexing the obtained X-ray diffraction patterns to assign the indices of all lines.

A transmission electron microscope (EM10, Zeiss) of resolving power 0.4 nm operating at 60 kV and an attached diffraction stage were also used for structural investigation of the samples in thin film form.

1.3 Electrical resistivity measurements

The two-point probe technique was used in electrical resistivity measurements at room temperature as well as elevated temperatures. Thick vacuum-deposited Al films at the two ends of the sample were used as ohmic contacts.

A high impedance ($10^{14} \Omega$) electrometer (Keithley 616) was used for resistance measurements.

1.4 Optical measurements

The transmittance, T , of the $\text{Cd}_x\text{Zn}_{1-x}\text{Se}$ thin films, deposited on quartz substrates, was measured at normal incidence using a double-beam spectrophotometer (Carry 2390, Varian Co.) provided with a microcomputer, in the wavelength range of 360–2000 nm.

For measuring the reflectance, R , of the film under investigation at normal incidence when the monochromatic light is incident on it through air, a specular reflection accessory is used with the aforementioned spectrophotometer.

2 Results and discussion

Structural analysis of the prepared ingots of the system $\text{Cd}_x\text{Zn}_{1-x}\text{Se}$ by X-ray diffractometry revealed the existence of two composition ranges. The first range extends from $x = 0$ to $x = 0.5$, where the solid solution was found to crystallize in the sphalerite-type crystal lattice. The second composition range extends from $x = 0.6$ to $x = 1$, where the solid solution was found to crystallize in the wurtzite-type crystal lattice. The prominent diffraction peaks in the X-ray diffractograms illustrated in Figs. 1 and 2 correspond to the (111), (220), and (311) reflecting planes of the sphalerite structure and to the (100), (101), (110), (112), and (002) reflecting planes of the wurtzite structure.

The calculated lattice parameters of the prepared ingots were found to vary with composition in a linear relation for each type of structure and showing a transition at about $x = 0.55$. Thus, the solid solutions showed a behaviour in accordance with Vegard's law for each crystal type, being continuous and homogeneous. The values of the lattice constants of the solid solutions lie between the corresponding values of the CdSe and ZnSe.

The analysis of X-ray diffractograms of the deposited films revealed a prominent peak corresponding to the (111) reflecting plane of the sphalerite-type lattice for films with $x = 0.1$ to $x = 0.5$. However a predominant diffraction peak corresponding to the (002) reflecting plane of the wurtzite type lattice was found for films with $x = 0.5$ to $x = 0.9$.

The relation between the d -spacing of the (111) reflecting plane of the sphalerite and the (002) plane of the wurtzite with composition revealed two straight lines extending into each other as shown in Fig. 3. This indicates that the deposited films are continuous solid solutions following Vegard's law, since the (002) reflecting plane of the wurtzite lattice is equivalent to the (111) plane of the sphalerite lattice. X-ray structural analysis and electron diffraction investigations of the film structure revealed [12] that when $x < 0.5$, the solid solution $\text{Cd}_x\text{Zn}_{1-x}\text{Se}$ had the sphalerite structure, but when $x > 0.7$ it had the wurtzite structure. In the range $0.5 < x < 0.7$, the epitaxial layers were found to contain both modifications. Using

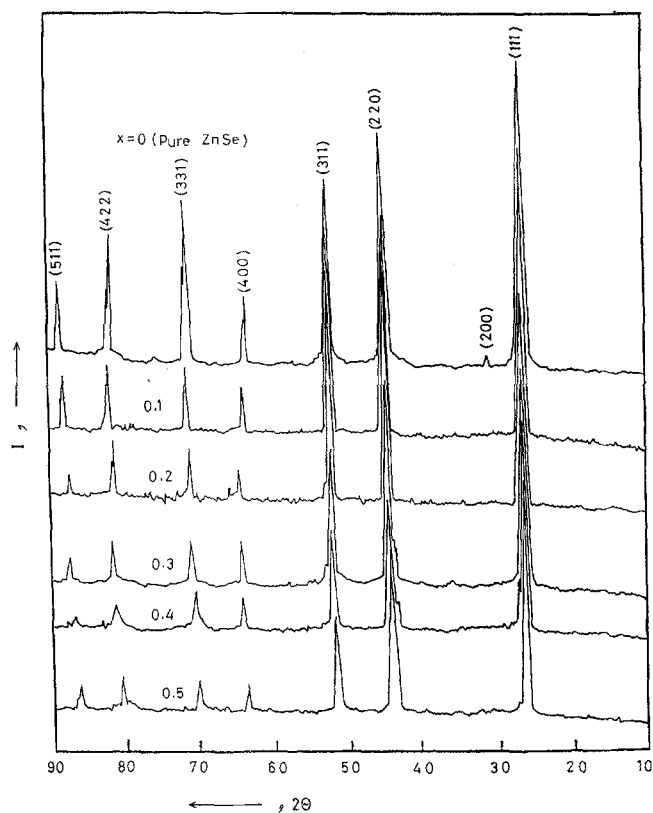


Fig. 1. X-ray diffraction of $\text{Cd}_x\text{Zn}_{1-x}\text{Se}$ ingots ($0 \leq x \leq 0.5$)

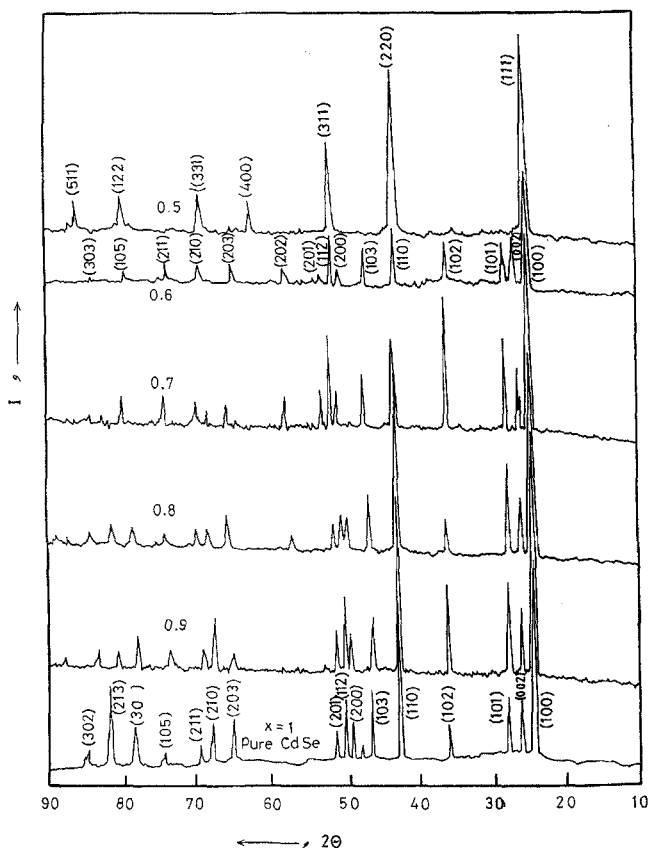


Fig. 2. X-ray diffraction of $\text{Cd}_x\text{Zn}_{1-x}\text{Se}$ ingots ($0.5 \leq x \leq 1$)

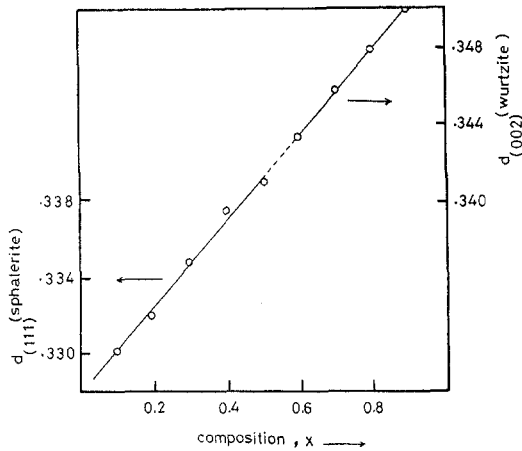


Fig. 3. Lattice-spacing (d) of (111) and (002) reflecting planes as a function of the molar fraction x

X-ray diffraction, it was shown [13] that up to about 30% molar concentration of CdSe, the mixture is sphalerite; it is wurtzite when the molar concentration of CdSe exceeds 50%. Between 30% and 50% CdSe, there exists a two phase region with an exact range depending on the growth temperature.

The crystallite size of the deposited films was found to increase with film thickness for each composition, as determined from the broadening of the X-ray diffraction peaks.

Transmission electron diffraction patterns of the deposited films were ring patterns as illustrated in Fig. 4a, b indicating that they are polycrystalline consisting of a random distribution of crystallites.

The analysis of electron diffraction patterns carried out for $\text{Cd}_x\text{Zn}_{1-x}\text{Se}$ thin films shows that the determined d -spacings are in agreement with that obtained from the analysis of X-ray diffraction patterns, revealing the existence of sphalerite phase in the mole range from $x = 0.1$ to $x = 0.5$ and wurtzite phase in the range from $x = 0.6$ to $x = 0.9$. The obtained data is in good agreement with that mentioned before [14].

The electrical resistivity of the deposited films was measured as a function of molar composition x in air as well as in vacuum. The room temperature dark electrical resistivity, shown in Fig. 5, varies with the compositions showing distinct regions, the first one for ($0.1 < x < 0.5$), the second one for ($0.6 < x < 1$). This was attributed to the transition from the sphalerite type to the wurtzite type as revealed by diffraction techniques.

It has been reported [14] that the reduction in the resistivity of the $\text{Cd}_x\text{Zn}_{1-x}\text{Se}$ films with the increase in x is caused by several factors. Firstly, the reduction in carrier concentration is due to vacancy formation in the metal sublattice, resulting in the compensation of the electron resistivity. Secondly, carrier scattering is amplified by both intercrystalline barriers and the local perturbation of the potential in the $\text{Cd}_x\text{Zn}_{1-x}\text{Se}$ lattice. The temperature dependence of the carrier mobility and concentration showed a high degree of compensation in the $\text{Cd}_x\text{Zn}_{1-x}\text{Se}$ layer and a decrease in the intracrystallite

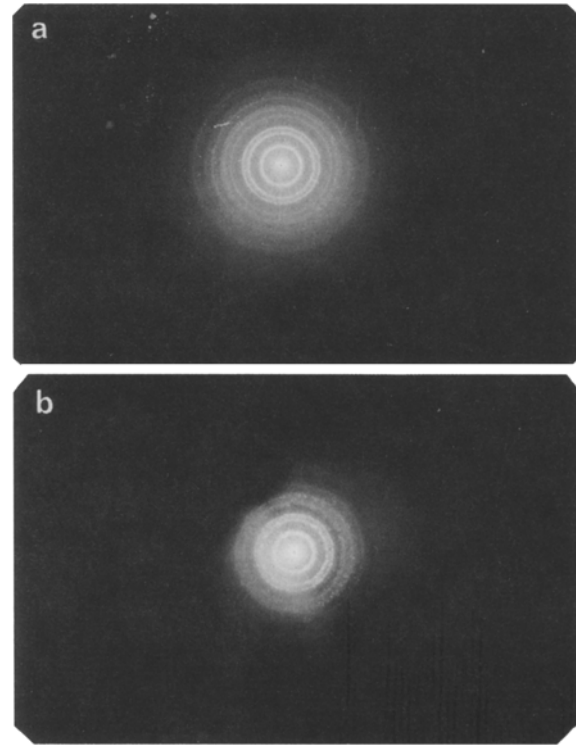


Fig. 4a, b. Electron diffraction pattern of $\text{Cd}_x\text{Zn}_{1-x}\text{Se}$ thin films (a) $x = 0.4$ and (b) $x = 0.8$

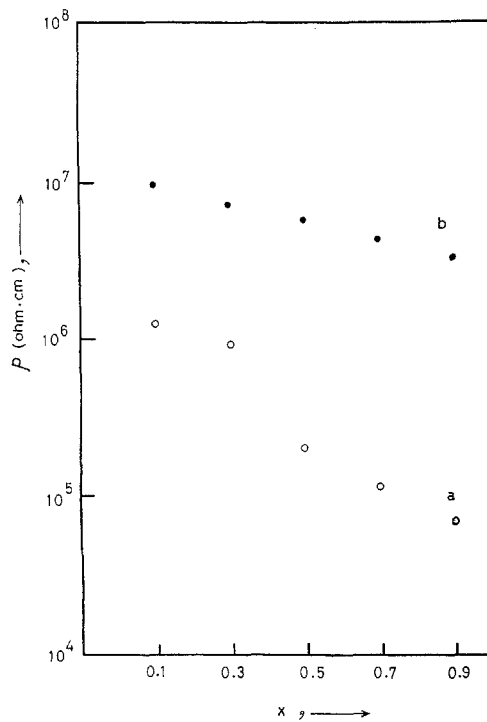


Fig. 5. Room temperature electrical resistivity ρ of $\text{Cd}_x\text{Zn}_{1-x}\text{Se}$ thin films vs x measured in air (curve a) and in vacuum (curve b)

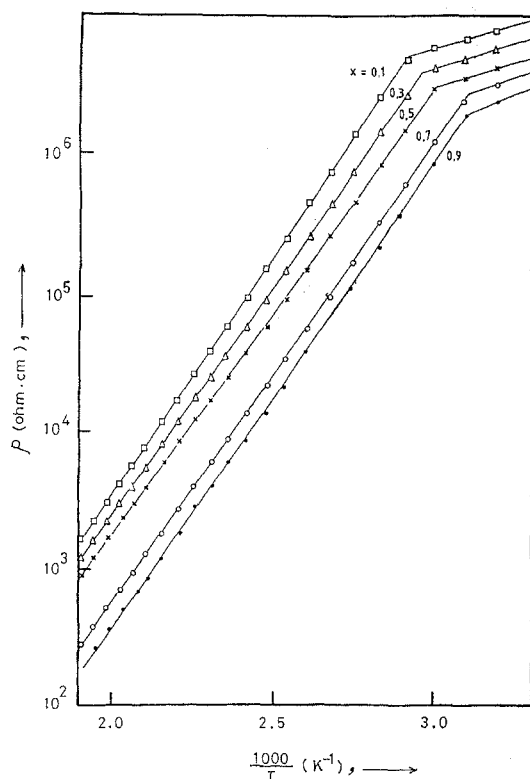


Fig. 6. The electrical resistivity ρ as a function of $1000/T$ for $\text{Cd}_x\text{Zn}_{1-x}\text{Se}$ thin films of different compositions

barrier with increasing x . The $\text{Cd}_x\text{Zn}_{1-x}\text{Se}$ films with $x < 0.5$ had a high specific resistivity.

The temperature dependence of the electrical resistivity of the deposited films illustrated in Fig. 6 revealed two conductivity mechanisms. One conduction mechanism, below about 352 K, is due to shallow-level surface states and defects introduced during the film growth. The other conduction mechanism, occurring above 352 K, is due to deep-level ionization, following the semiconducting relation.

$$\rho = \rho_0 \exp (\Delta E/k_B T)$$

where ΔE is the activation energy and k_B is Boltzmann's constant. The temperature corresponding to the kink in $\log \rho$ vs $(1/T)$ plot was found to vary with the molar fraction x . For films with $x = 0.1$ to $x = 0.5$, the activation energy of the charge carriers was found to decrease linearly with x . Above $x = 0.5$, the activation energy was found to increase with x . This could be correlated to the transition from the sphalerite-type crystal structure to the wurtzite-type crystal structure.

Spectrophotometric measurements of the transmittance and reflectance at normal incidence of light in the range 360–2000 nm for thin films of $\text{Cd}_x\text{Zn}_{1-x}\text{Se}$ deposited on pre-cleaned quartz and glass substrates were used for determining the optical constants of the corresponding films.

A computer program based on exact formulas representing both T and R was used to obtain the absolute values of refractive index, n , and absorption index, k , for different wavelengths [15].

The real and imaginary parts of the complex refractive index, $\tilde{n} = n - ik$, were determined for different compositions. The dispersion curves shown in Fig. 7 indicate that at the long wavelengths, the refractive index decreases with composition up to $x = 0.6$, above which the value of the refractive index increases.

The spectral behaviour of the absorption index illustrated in Fig. 8 revealed that the absorption edge shifts to the long wavelength side as x increases. The analysis of the absorption coefficient at and near the absorption edge indicated allowed optical transitions, where the energy gap was found to decrease on increasing the molar fraction x , i.e., as the CdSe content increases. The spectral curves obtained for the CdSe–ZnSe system showed [16] that a gradual shift in spectral response occurred with a change in composition. The variation in the activation energy was smooth, without any indication of a discontinuity. The nature of the spectral response in the fundamental absorption region depended on the structure type of the substance.

The optical activation energy at room temperature of thin layers of CdSe–ZnSe system was found to vary in the range 2.6–1.7 eV depending on the molar fraction x of the binary compound [17]. The forbidden-band width was determined [18] from the transmission spectra of the condensate specimens of CdSe–ZnSe solid solution.

The variation of E_g^d with the CdSe content (x) for the system $\text{Cd}_x\text{Zn}_{1-x}\text{Se}$ in the present work was found to be of the form

$$E_g^d = 2.592 - 1.638 x + 0.730 x^2,$$

which is completely different from that equation presented by Krestovnikov et al. [18] in the following form:

$$E_g^d = 2.568636 + 0.22422 x + 0.000398 x^2 + 0.00004 x^3.$$

However, the relation obtained in this work indicated that $\text{Cd}_x\text{Zn}_{1-x}\text{Se}$ solid solution in thin film form belongs to the amalgamation type with bowing parameters $a \approx 1.638$ and $b = 0.730$.

Acknowledgements. The authors express their sincere gratitude and appreciation to Prof. M. M. El-Nahass, for fruitful discussions during the course of this work.

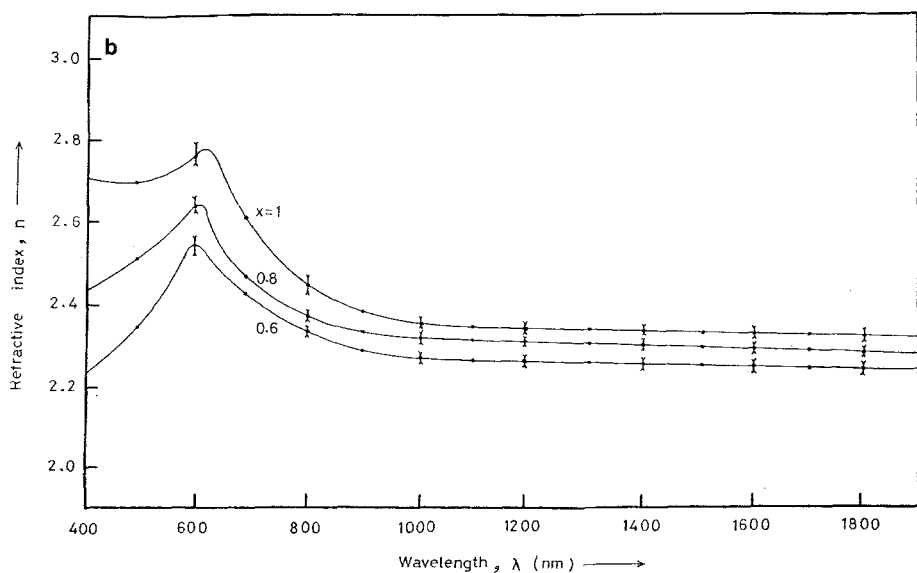
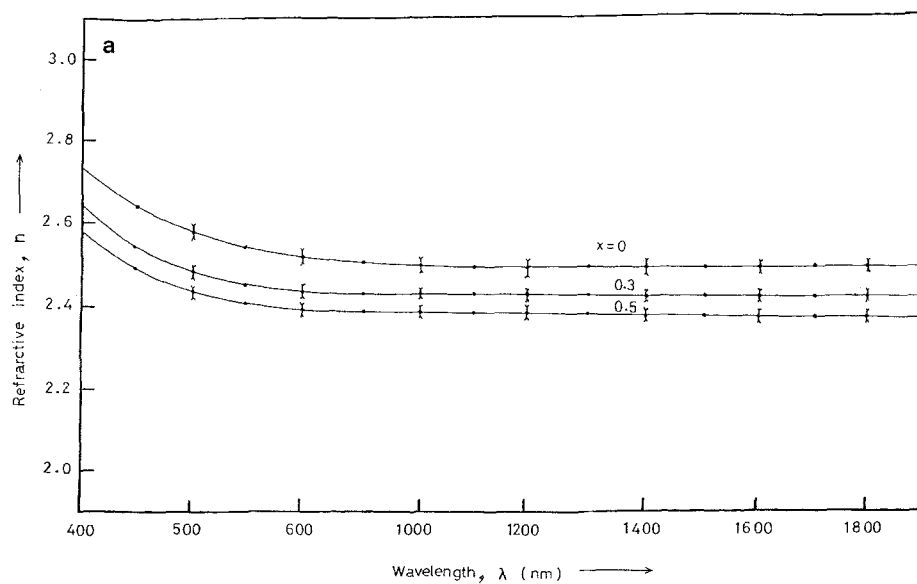


Fig. 7a, b. Refractive index n vs for $\text{Cd}_x\text{Zn}_{1-x}\text{Se}$ thin films: (a) $0 \leq x \leq 0.5$ and (b) $0.6 \leq x \leq 1$

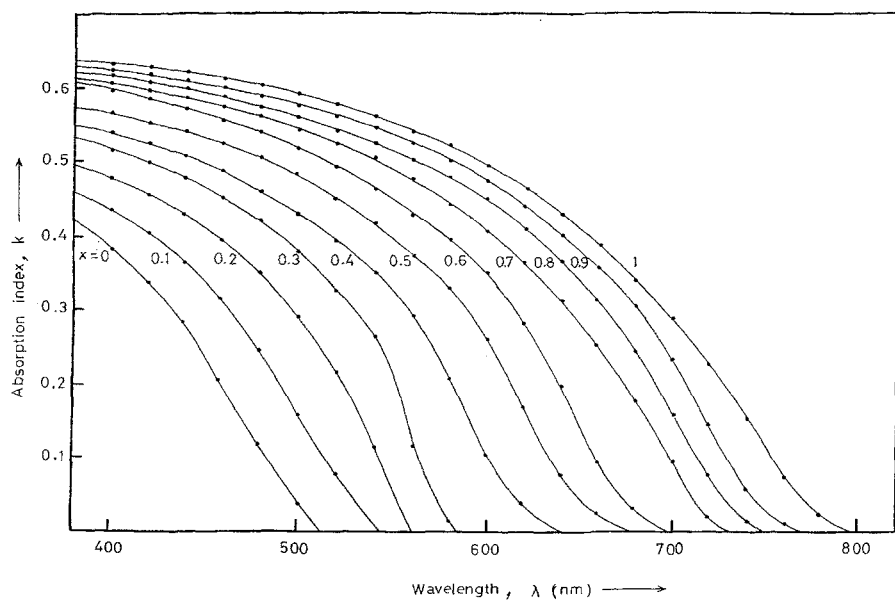


Fig. 8. The absorption index k vs λ for $\text{Cd}_x\text{Zn}_{1-x}\text{Se}$ thin films of different compositions

References

1. R.K. Willardson, A.C. Beer: *Semiconductors and Semimetals*, Vol. 5 (Academic, New York 1970)
2. C.E. Hurtz: *Appl. Phys. Lett.* **8**, 121 (1966)
3. S.V. Svechnikov, E.B. Kaganovich: *Thin Solid Films* **66**, 41 (1980)
4. B. Ray: In *II-VI Compounds* (Pergamon, London 1969) p. 172
5. N.I. Vitrikhovskii, I.B. Mizetskaya: *Sov. Phys.-Solid State* **1**, 358 (1959)
6. M. Aven, J.S. Prener: In *Physics and Chemistry of II-VI Compounds* (North-Holland, Amsterdam 1967) p. 613
7. R.J. Phelan: *IEEE Proc.* **54**, 1119 (1966)
8. M. Aven: *Appl. Phys. Lett.* **7**, 146 (1965)
9. F.F. Morehead, G. Mandel: *Appl. Phys. Lett.* **5**, 53 (1964)
10. S. Tolansky: In *Multiple-Beam Interference Microscopy of Metals* (Academic, London 1970) 55
11. B.D. Cullity: *Elements of X-ray Diffraction*, 2nd edn. (Addison Wesley, New York 1978) p. 327
12. V.A. Sanitarov, Yu.K. Ezhovskii, I.P. Kalinkin: *Inorg. Mater.* **12**, 1584 (1976)
13. K.V. Shalimova, A.F. Botnev, V.A. Dmitriev, N.Z. Kognovitskaya, V.V. Starostin: *Sov. Phys. Cryst.* **14**, 531 (1970)
14. V.A. Sanitarov, Yu.K. Ezhovskii, I.P. Kalinkin: *Sov. Phys. J.* **1**, 62 (1976)
15. M.M. El-Nahass, H.S. Soliman, N. El-Kadry, A.Y. Morsy, S. Yaghmour: *J. Mater. Sci. Lett.* **7**, 1050 (1988)
16. B.T. Kolomiets, Lin Chun-ting: *Sov. Phys.-Solid State* **2**, 154 (1960)
17. M.V. Kot, V.G. Tyrziu, A.V. Simashkevich, Yu.E. Maronchuk, V.A. Mshenskii: *Sov. Phys.-Solid State* **4**, 1128 (1962)
18. A.N. Krestovnikov, T.A. Valkova, A.F. Mikheenkova, I.A. Timoshin: *Inorg. Mater.* **11**, 811 (1975)